

Application of clay as a sustainable building material. Characteristics of ancient clay plasters – pilot results

Katerina Mihaylova^{1,3}, Ventsislava Ivanova², Bilyana Kostova¹

¹New Bulgarian University, Department of Natural sciences, 21 “Montevideo” Str., Sofia, Bulgaria

²New Bulgarian University, Department of Archaeology, 21 “Montevideo” Str., Sofia, Bulgaria

³Institute of Mineralogy and Crystallography “Acad. Ivan Kostov” – Bulgarian Academy of Sciences, 107 “Acad. Georgi Bonchev” str., Sofia, Bulgaria

kate.wess17@gmail.com

Приложение на глината като устойчив строителен материал. Характеристика на древни глинени мазилки – пилотни резултати

Катерина Михайлова^{1,3}, Венцислава Иванова², Биляна Костова¹

¹Нов български университет, департамент “Природни науки”, “бул. Монтевидео” № 21, София България

²Нов български университет, департамент “Археология”, “бул. Монтевидео” № 21, София България

³Институт по минералогия и кристалография “Акад. Иван Костов” – Българска академия на науките, ул. “Акад. Георги Бончев” 107, София, България

kate.wess17@gmail.com

Abstract: Clay is a popular traditional material that has been used for the construction of building materials and household objects since time immemorial. Due to its plastic property and capacity to regulate humidity, it was often used in the form of clay plasters. At present, the building sector has become a serious contributor to climate change, thus triggering a need for the use of more sustainable and eco-friendly materials. This paper aims to analyze the characteristics of ancient clay plasters from the Roman age and define their production technology. The reason for this study is that the ancient production recipes of clay plasters are the base for the modern ones. The analytical methods that were used in this research include X-ray fluorescence (XRF) analysis, Powder X-Ray diffraction (PXRD) analysis, Fourier transformed infrared (FTIR) measurements and thermal analysis. It was established that two types of raw clay were used for the clay plasters’ preparation, calcareous and non-calcareous, and both match the rock types on the surface around the archeological sites, meaning that the clay was most likely of local origin. There are no signs of burning on the samples; however there is a high probability that they were intentionally treated thermally within a similar temperature range. The acquired results suggest a good environmental knowledge throughout the Roman era and an ability to work well with traditional materials, but with different properties. The results are also of practical value, since they can be applied in the creation of modern plasters that can be used both in modern buildings and for conservation and restoration purposes.

Key words: clay (earthen) plaster, sustainable development, eco-friendly building materials.

Резюме: Глината е популярен традиционен материал, който се е използвал за създаването на строителни материали и предмети за бита от древни времена. Поради пластичните си свойства и способността си да регулира влажността, често се е използвала под формата на глинени мазилки. Понастоящем строителният сектор се е превърнал в

сериозен фактор за изменението на климата, което от своя страна създава необходимост от използването на по-устойчиви и екологични материали. Тази статия има за цел да анализира характеристиките на древни глинени мазилки от римската епоха и да определи технологията на тяхното производство. Причината за това проучване е, че древните рецепти за производство на глинени мазилки са основа на съвременните. Аналитичните методи, използвани в това изследване, включват рентгенов флуоресцентен анализ (XRF), прахова рентгенова дифракция (PXRD), инфрачервена спектроскопия (FTIR) и термичен анализ. Установено е, че за приготвянето на глинени мазилки са използвани два вида изходна глина – варовита и неваровита, като и двете съвпадат с видовете скали на повърхността около археологическите обекти, което означава, че глината най-вероятно е с местен произход. Няма следи от опожаряване по пробите, което предполага, че са умишлено термично третираны в близък температурен диапазон. Получените резултати предполагат добро познаване на околната среда през римската епоха и умение за работа с традиционни, но различаващи се по свойства материали. Резултатите имат и практическа стойност, тъй като могат да бъдат приложени при създаването на съвременни мазилки, които да се използват както в съвременното строителство, така и за консервационни и реставрационни цели.

Ключови думи: глинена мазилка, устойчиво развитие, екологично чисти строителни материали.

Introduction

Clays are natural formations, made out of clay minerals, accessory minerals and impurity minerals. Clay minerals include kaolinites, montmorillonites, and illites, accessory minerals – micas, chlorites, vermiculites, and impurity minerals – quartz, feldspars, calcite, iron minerals, etc [Meyers, 2003]. Depending on the CaO content in the clays, they can be categorized as two different types – calcareous and non-calcareous. Clays that contain more than 5% CaO are defined as calcareous [Badica et al., 2022].

The application of clay in the construction of buildings has been done since ancient times. In the past, people used clay to make plasters, bricks, tiles, etc [Liskova et al., 2016]. Bricks, tiles and household ceramics are produced by firing at temperatures from 300 to 1050 °C [La Noce et al., 2021]. The baking process leads to a change in the clay's characteristics, giving it properties such as strength and resistance. When the clay is heated to ~ 600 °C (firing stage), the processes of dehydration, oxidation and/or dehydroxylation occur in a consecutive order. At temperatures above 600 °C (baking stage), the processes of dehydroxylation and decarbonization take place. At temperatures above ~ 850 °C (burning stage) the processes of crystallization of high-temperature phases are carried out [Goffer, 2007]. This crystallization can occur both from a melt (after vitrification of the material) and in solid state through recrystallization. The method of formation of the high-temperature phases depends on the chemical composition of the raw clay and the temperature of the clay's thermal treatment [Aras et al., 2018, Badica et al., 2022], which also determines the quality of the ceramic artifacts and their manufacturing process [Emmami et al., 2016].

For the classic production of clay (earthen) plasters, the components that are used include dried clay, sand (if the sand fraction in the clay is in low quantity) and organic material (straw, for example), after which water is added to them. Clay gives plasticity to the plaster, sand – strength, and the organic material holds the plaster together and provides some flexibility to the plaster once it is dried [Ma et al., 2018; Melià et al., 2014]. Clay plasters are better applied in the internal layer of the building and can be used on various types of wall bases, such as concrete,

bricks, wood, straw bales, rammed earth, etc. Such indoor plasters serve as ideal moisture regulators due to the clay's high absorption capacity. They ameliorate the quality of life by creating better indoor conditions, such as improved humidity levels, warmer temperatures in winter and cooler temperatures in summer [Emiroglu et al., 2015]. This however decreases significantly the material's water resistance potential, so in order to be used for the external part of a structure, additional hydrophobizing additives may need to be mixed into the clay [Liskova et al., 2016]. External clay plasters can be used for restoration purposes such as the reconstruction of historical buildings' façades [La Noce et al., 2021].

Nowadays the building sector has become one of the main pollutants that contribute to climate change. As industries grow, so does their need for better infrastructure. Modern structures need to be more sustainable and eco-friendly, while still being long-lasting and of good quality. In order to achieve this, the same clay-based products that were used in ancient times can be applied today. Their use would be even more successful, since they can serve as a substitute for products with a higher environmental impact. It should be noted that while no material is ever 100% eco-friendly, natural substances such as clay are a lot more “eco-efficient” than a conventional material that would require additional production processes [La Noce et al., 2021]. Conventional plasters are cement plasters, lime plasters and hydraulic lime plasters. Cement plasters are a mixture of sand and Portland cement and lime plasters are made out of sand and calcium hydroxide, with the difference that the hydraulic plaster contains impurities in the calcium hydroxide, which enable the lime to set without air exposure. Conventional plasters generate a lot more CO₂ emissions than the earthen ones. One m² of cement base plaster produces 5.86 kg CO_{2eq}, while hydraulic lime plaster produces 6.37 kg CO_{2eq}, which is 6 times more than the emissions of an earthen base plaster - 0.88 kg CO_{2eq}. [Melià et al., 2014]. In addition, a lot more energy and resources are saved by using materials that are locally available and easily produced [La Noce et al., 2021].

The goal of this work is to characterize ancient types of clay plasters from the Roman age which were obtained from Bulgarian archeological sites. The reason for this study is that the production recipes of modern plasters are based on the ones of ancient plasters. The samples were analyzed with X-ray fluorescence (XRF) analysis, Powder X-Ray diffraction (PXRD) analysis, Fourier transformed infrared (FTIR) measurements and thermal analysis.

The acquired results are of fundamental and practical value for the sustainable development of modern construction materials and for the reconstruction of the ancient environment.

1. Materials and methods

Sample No. 62 clay wall plaster (Fig. 1) from archaeological site No. 8 Dimitriev, Emporion Pizos, Roman age [Boyanov, 2014]. The plaster is coloured in orange-red. Imprints of organic material are observed on the plaster's surface. Pores with irregular shape are found on the inside of the plaster. Some of them have black coal particles. No signs of burning have been found at the archaeological site.

Sample No. 83 clay wall plaster (Fig. 2) from archaeological site No. 6 Malko Tranovo - open settlement, Roman vicus [Dumanov, 2005]. The plaster has a bright yellow colour. Traces of organic material are observed on the plaster's surface. Pores with irregular shape are found inside the plaster. No signs of burning have been found at the archaeological site.



Fig. 1. Sample No. 62 clay wall plaster



Fig. 2. Sample No. 83 clay wall plaster

X-ray fluorescence (XRF) analysis was performed by energy dispersive Micro-XRF Spectrometer M1 MISTRAL, Bruker (Rh-tube, Peltier cooling, 30 mm², Si-drift detector (SDD), MnK α resolution <150 eV, collimator 0.1 mm to 1.5 mm). The samples were prepared as pressed pellets with (CEREOX-BM-0002-1 powder) (1.00 g sample + 0.15 g CEREOX- BM-0002-1 powder).

The powder X-ray diffraction (PXRD) measurements were made by D2 Phaser BrukerAXS, CuK α radiation ($\lambda = 0.15418$ nm) (operating at 30 kV, 10 mA) from 3 to 70 °2 θ with a step of 0.05°, 1 s/step (ground sample weight – 1.0 \pm 0.1 mg and particle size below 0.075 mm). The PDF [PDF, 2001] database was used for determining the phases and minerals in the samples.

Fourier transform infrared (FTIR) measurements were performed by FTIR Spectrometer Nicolet 6700, covering the range of 400 - 4000 cm⁻¹ with 100 scans and 1.928 cm⁻¹ resolution. The samples were prepared as pellets with KBr.

Thermal analysis: simultaneous TG/DTG-DSC analysis was carried out on a Setline STA 1100, SETARAM, France, in the temperature range room temperature (RT) – 1050°C; in static air, with a heating rate of 10°C min⁻¹. The operational characteristics of the TG/DTG–DSC - system were: sample mass of 25.0 \pm 1.0 mg (mass resolution of 0.05 μ g), temperature resolution of +/- 0.3°C, and alumina sample crucible with a volume of 100 μ L.

2. Results and discussion

2.1. XRF

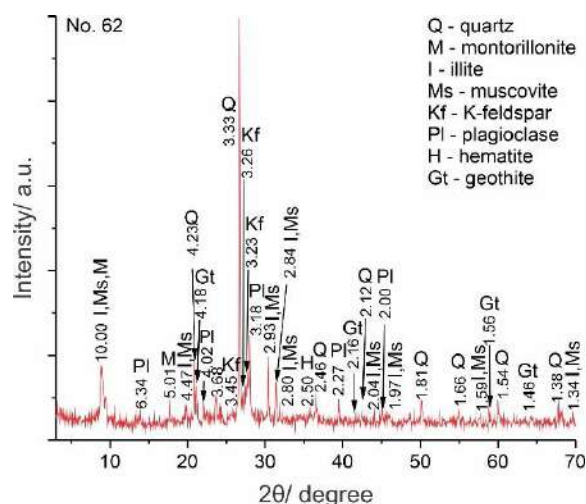
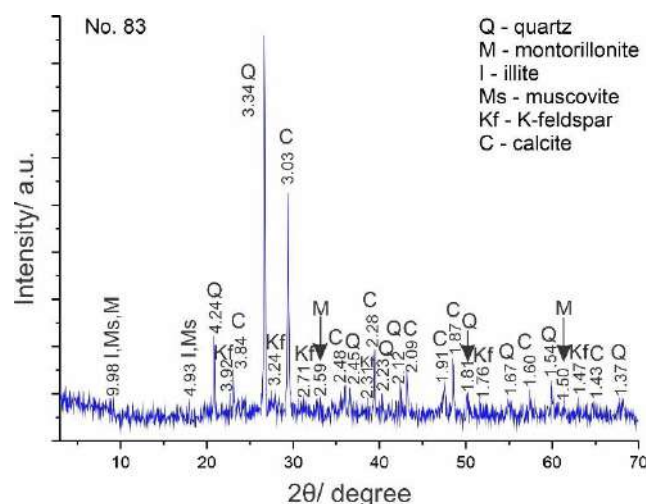
The results from the XRF analysis are presented in Table 1. The SiO₂ content is the highest in both samples. The content of Al₂O₃ is also high, which suggests the presence of silicates and aluminosilicates in the samples. A CaO content of 34.17% was measured in sample No. 83 and in sample No. 62 - 2.81%. Both samples are likely to form carbonates (carbonates are a frequent impurity in clays in amounts from parts of a percent to 30-40%), Ca-plagioclases (anorthite), calcium clay minerals from the montmorillonite group [Chamley, 1989]. The K₂O content suggests the formation of potassium aluminosilicates. The Fe₂O₃ content indicates the presence of individual iron phases and/or iron incorporated into aluminosilicate minerals. The remaining elements are in low concentrations and probably do not form their own phases.

Table 1. XRF results (mass %)

Sample	Na ₂ O	MgO	Al ₂ O ₃	SiO ₂	P ₂ O ₅	SO ₃	K ₂ O	CaO	TiO ₂	MnO	Fe ₂ O ₃
No. 62	1.20	1.82	20.42	62.91	0.42	-	4.54	2.81	0.59	0.11	5.06
No. 83	0.15	1.01	13.05	42.18	0.38	0.11	1.76	34.17	0.59	0.14	5.68

2.2. PXRD

The PXRD results are shown in Figs. 3, 4. Both samples contain quartz SiO₂ (#06-1757), montmorillonite (Na,Ca)(Al,Mg)₂(Si₄O₁₀)(OH)₂nH₂O (#302-0239), illite (K_{0.65}Al₂[Al_{0.65}Si_{3.35}O₁₀](OH)₂ (#25-0001), muscovite KAl₂(AlSi₂O₁₀)(OH)₂ (#34-0175), potassium feldspar - microcline, KAlSi₃O₈ (#84-0710). Plagioclase - albite NaAlSi₃O₈, (#89-6426), hematite Fe₂O₃ (#72-0469) and goethite Fe³⁺O(OH) (#29-0713) in sample No. 62, and calcite, CaCO₃ (#47-1743) – in sample No. 83.

**Fig. 3.** PXRD pattern of sample No. 62.**Fig. 4.** PXRD pattern of sample No. 83.

2.3. FTIR

The FTIR results (Figs. 5, 6 and Table 2) confirm the PXRD results, while also giving additional information regarding the inorganic and organic phases in the studied samples. The following inorganic phases have been proved, which match the ones determined by PXRD (Table 2):

- muscovite and illite in both samples.
- hematite and goethite – only in sample No. 62.
- quartz, montmorillonite and potassium feldspar – in both studied samples.

Additionally, the following phases have been established – calcite in sample No. 83, albite and magnetite – in both samples. These phases were not registered through PXRD due to the low limits of detection of the method – 5% [Moropoulou et al., 1995].

Through FTIR, both samples were proven to have:

- surface adsorbed water (moisture).
- organic phases.

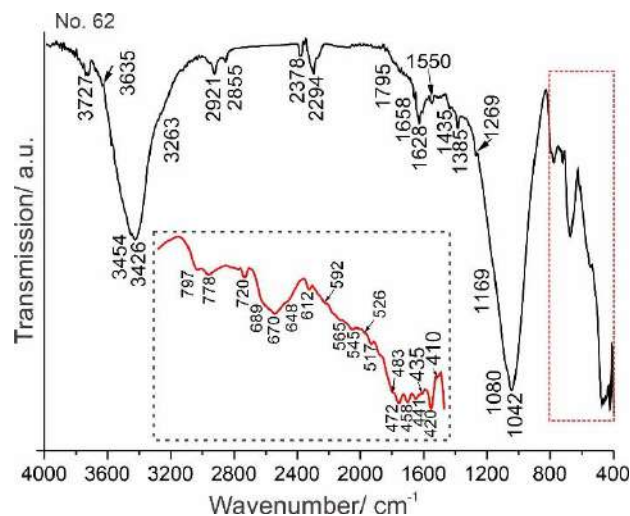


Fig. 5. FTIR spectrum of sample No. 62.
Insertion: 860-400 cm⁻¹ spectral range.

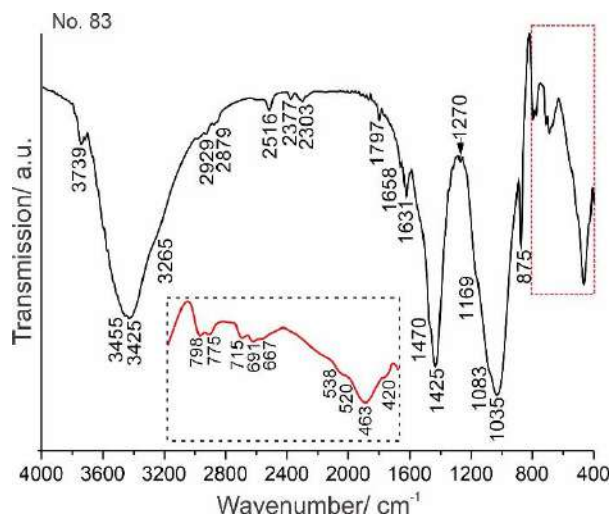


Fig. 6. FTIR spectrum of sample No. 83.
Insertion: 860-400 cm⁻¹ spectral range.

Table 2. FTIR results

Wavenumber/cm ⁻¹		Assignment	References
No. 62	No. 83		
3727	3739	O-H from the air (surface hydroxils)	Chukanov, Chervonnyi, 2016; Jozanikohan et al., 2022
3635	-	Al-OH stretching band of illite montmorillonite	Chukanov, 2014, Yan et al., 2021
3454	3455	H-O-H stretching vibration of adsorbed water molecules in illite	Chukanov, 2014; Jozanikohan, 2022
3426	3432	H-O-H stretching vibration of adsorbed water molecules in illite	Chukanov, 2014, Jozanikohan et al., 2022
3263	3265	Metal-O-H stretching vibration of montmorillonite	Caccamato, 2020
2921	2929	C-H asymmetrical stretching vibrations of CH ₂	Silva et al., 2005; Rao et al., 2017
2855	2879		
-	2516	(ν ₁ + ν ₃) C-O in CO ₃ ²⁻ of calcite	Chukanov, 2014
2378	2377	CO ₂ from the air	Theophanides, 2012; Chukanov, Chervonnyi, 2016
2294	2303		
1795	1797	(ν ₁ + ν ₄) C-O in CO ₃ ²⁻ of calcite	Chukanov, 2014; Stanienda et a., 2016
1658	1658	O-H bending vibration of adsorbed water molecules of illite	Chukanov, 2014
1628	1631	O-H stretching vibration of adsorbed water molecules of illite and muscovite	Chukanov, 2014, Singha, 2016
1550	-	Skeletal vibrations of the aromatic ring from lignin	Rao et al., 2017

-	1470	ν_3 C-O in CO_3^{2-} of calcite	Chukanov, 2014
1435	1425	ν_3 C-O in CO_3^{2-} of calcite	Chukanov, 2014
1385	-	C-H bending vibrations of the methyl and methylene group	Rao et al., 2017
1269	1270	ν_3 stretching vibration of C-O in aromatic rings	Rao et al., 2017
1169	1169	ν_3 Si-O in SiO_2 in quartz	Chukanov, 2014
1080	1083		
1042	1035	Si-O-Si vibration band of illite and montmorillonite	Chukanov, 2014, Yan et al., 2021
-	875	ν_2 C-O in CO_3^{2-} of calcite	Chukanov, 2014
797	798	ν_2 Si-O in SiO_2 in quartz	Chukanov, 2014
778	775		
-	715	ν_4 C-O in CO_3^{2-} of calcite	Chukanov, 2014
720	-	ν Si(Al)-O stretching vibration in albite	Chukanov, 2014
692	691	ν_1 Si-O in SiO_2 in quartz	Chukanov, 2014
689	-	ν Si(Al)-O stretching vibration in montmorillonite	Chukanov, 2014
670	667	Fe^{3+} -O vibration at magnetite	Ravisankar et al., 2010; Chukanov, 2014
648	-	Fe^{3+} -O vibration at hematite	Chukanov, 2014; Jozanikohan et al., 2022
612	-	O-Si(Al)-O bending vibrations albite	Theodosoglou et al., 2010; Chukanov, 2014
592	-	O-Al-O bending vibration at albite	Chukanov, 2014
565	-	O-Al-O bending vibration at microcline	Chukanov, 2014,
545	538	O-Si-O deformation the K-O stretching at albite	Chukanov, 2014
526	520	Al-O-Al vibration at illite	Chukanov, 2014; Yan et al., 2021
517	-	Al-O-Al vibration at muscovite	Chukanov, 2014; Yan et al., 2021
483	-	Si-O-Si deformation at albite	Chukanov, 2014
472	-	Si-O-Si bending and the K-O stretching vibrations in muscovite, illite and montmorillonite	Chukanov, 2014
-	463	O-Si-O bending and the K-O stretching vibrations in microcline	Theodosoglou et al., 2010; Chukanov, 2014
458	-	Fe^{3+} -O hematite vibration	Chukanov, 2014
441	-	O-Si-O bending and the K-O stretching vibrations in microcline	Chukanov, 2014
435	-	Si-O bending vibration of illite	Chukanov, 2014
420	420	Si-O-Si deformation in microcline	Theodosoglou et al., 2010;

			Chukanov, 2014
410	-	Fe-O goethite vibration	Chukanov, 2014

2.4. Thermal analysis

The thermal analysis results are presented in Figs. 7, 8 and Table 3. The total mass loss (ML_{tot}) when heating to 1050°C is 6.60% for sample No. 62 and 18.93% for sample No. 83. Five temperature ranges were determined: RT-220°C, 220-420°C, 420-720°C, 720-840°C, and 840-1050°C.

RT-220°C – dehydration

The stage is divided in two (Table 3):

- until 100°C – separation of hygroscopic water [Moropoulou et al., 1995]. The ML for sample No. 62 is 1.00% and for sample No.83 – 3.06%.
- between 100 and 220°C – a process of dehydration of phyllosilicates occurs – muscovite and illite [Meyers et al., 2003]. The ML in this range is 1.00% for sample No. 62, and 2.50% for sample No.83.

220-420°C organic decomposition

Combustion of organic matter occurs between 220 and 420°C [Palanivel et al., 2011]. The exo effect of organic decomposition is at 344.9°C for No. 62 (Fig. 7), and 317.5°C for No. 83 (Fig. 8), while the ML is shown in Table 3.

Dehydroxylation of synthetic goethite also occurs during this temperature range, at $T_{infl} = 270^\circ\text{C}$ with a clearly pronounced peak. In naturally occurring goethite, the dehydroxylation peak is barely noticeable and is shifted towards 300°C, probably due to isomorphic inclusions in the mineral. After the dehydroxylation, goethite transforms into hematite [Trindade et al., 2009; Ponomar, 2018]. Goethite was found in wall plaster No. 62, while no dehydroxylation peak of goethite was observed in the DTG curve (Fig. 7), probably due to the low amount of the mineral in the sample.

420-720°C dehydroxylation

During this temperature range, dehydroxylation of phyllosilicates occurs. At 450-460°C, montmorillonite dehydroxylates [Brown, 2003; Laufek et al., 2021]. At 528-580°C, illite dehydroxylates [Hatakeyama, 1998; Földvári, 2011; Marsh et al., 2018]. At temperatures 660-700°C, muscovite dehydroxylates [Velosa et al., 2007; Földvári, 2011; Pei et al., 2018] (Table 3). After dehydroxylation, these minerals form stable dehydroxylated phases which preserve the original crystal structure of the raw minerals up until reaching a temperature above 800°C, when their structure breaks down [Lee et al., 2008].

Apart from dehydroxylation, two other thermal processes are registered. The first one is recognized as magnetite oxidation [Földvári, 2011]. It is observed with an exothermic peak of the DSC curve at 511.2°C (No. 62) and 477.3°C (No. 83) and a peak in the DTG curve with T_{infl} from 483.1°C (No. 62) and 443.0°C (No. 82) (Figs. 7, 8). The second process occurs without ML and with a peak on the DSC curve, positioned at 571.7°C for both samples (Figs. 7, 8). It is recognized as a polymorphous transition from α to β quartz [Moropoulou et al., 1995].

720-840°C decarbonation

Calcite decarbonization is established in the temperature range 720-840°C [Böke et al., 2006] (Table 3, Figs. 7, 8), which occurs at very similar temperatures in both samples - $T_{infl} = 811.8^{\circ}\text{C}$ (No. 63) and 808.4°C (No. 83). The CaCO_3 quantity in both samples is measured from the ML_{CO_2} (Table 3) – for sample No. 62, it is 0.9%, which explains why this phase is not registered through PXRD and only through FTIR and thermal analysis. The measured CaCO_3 quantity for sample No. 83 is 20.8%

840-1050°C structure destruction

The structures of illite, muscovite and montmorillonite break down in this temperature range. Illite's structure breaks down at $T_{infl} = 892.2^{\circ}\text{C}$ (No. 83) and 902.9°C (No. 63) (Table 3). An exothermic effect appears right after this process (A DSC curve peak at 936.0°C for No. 62 and at 907.5°C for No. 83 and (Figs. 7, 8), which is associated with the crystallization of high-temperature phases [Grim et al., 1940; Meyers et al., 2003; El Ouahabi et al., 2015]. The breakdown of muscovite's structure is registered at T_{infl} from 919.8°C to 973.8°C and at 973.8°C , and montmorillonite's – at 1010.3°C (No. 62), and 1015.9°C (No. 83) (Table 3) [Hatakeyama, 1998; Földvári, 2011]. Exothermic peaks are also registered after the breakdown of these minerals (Figs. 7 and 8), which can be associated with the crystallization of high-temperature phases as well [El Ouahabi et al., 2015, Kornilov, 2005]. In sample No. 83, which is also made out of clay with high calcite content, it is likely that high-temperature phases such as gehlenite, anorthite, wollastonite, cristobalite are formed [El Ouahabi et al., 2015]. In sample No. 62 (made out of minimal calcite content) it is likely that mullite, spinel-type phases and cristobalite crystallize at 1015.3°C (No. 62) and 1009.3°C (No. 83) [Kornilov, 2005; Lee et al., 2008]. For sample No. 83, mullite crystallization is not expected because the increased amount of CaO from the calcite decomposition prevents its crystallization [El Ouahabi et al., 2015].

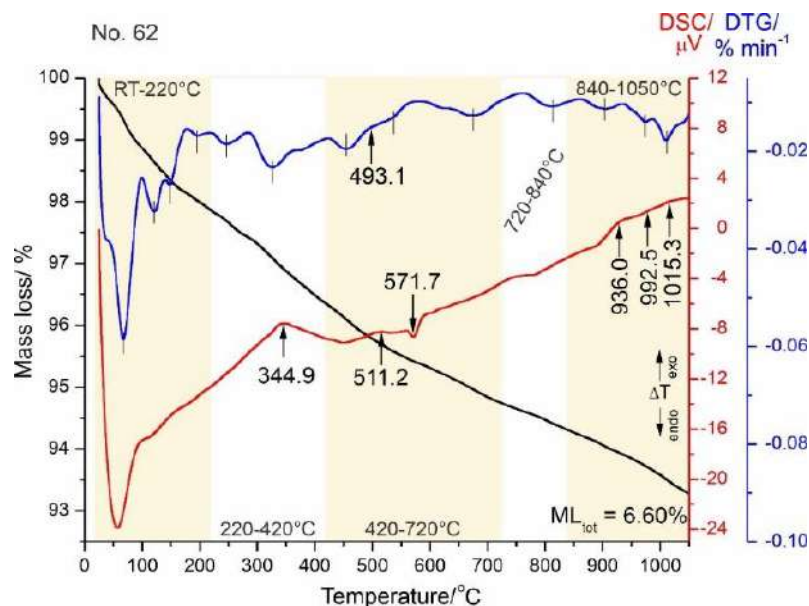


Fig. 7. TG/DTG-DSC of sample No. 62

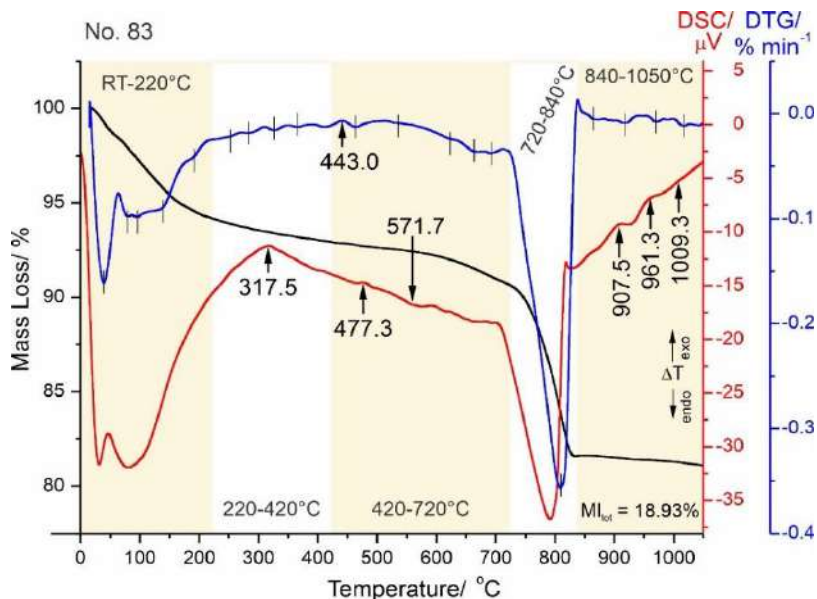


Fig. 8. TG/DTG-DSC of sample No. 83

Table 3. Thermal analysis results

Sample	RT-220°C dehydration				220-420°C organic decomposition		420-720°C dehydroxylation		720-840°C decarbonation		840-1100°C structure destruction	
	T _{infl} / °C	ML/ %	T _{infl} / °C	ML/ %	T _{infl} / °C	ML/ %	T _{infl} / °C	ML/ %	T _{infl} / °C	ML/ %	T _{infl} / °C	ML/ %
No. 62	67.1	1.00	120.7	0.44	245.9	0.46	454.1	0.59	811.8	0.40	902.9	0.31
			147.5	0.30	325.1	1.09	534.1	0.34			973.8	0.25
			194.7	0.26			674.2	0.80			1010.3	0.41
No. 83	39.5	1.56	137.9	1.78	252.2	0.35	463.1	0.20	808.4	9.19	869.2	0.04
	79.7	0.76	191.6	0.72	286.1	0.28	535.0	0.20			919.8	0.18
	94.9	0.74			326.8	0.22	623.1	0.38			970.5	0.04
					366.5	0.13	662.8	0.50			1015.9	0.07
							691.2	0.51				

Discussion

The chemical and phase composition of the wall plasters shows that they are made from two different types of clay. Sample No. 62 is prepared from non-calcareous clay with the main minerals being montmorillonite, illite, quartz, muscovite and secondary minerals goethite, hematite, magnetite, potassium feldspar, plagioclase, calcite. The hematite may have been a mineral that was part of the raw clay, or it may have been a secondary phase that was formed in the plaster [El Ouahabi et al., 2015]. Sample No. 83 – calcareous clay with the main minerals being montmorillonite, illite, muscovite, quartz, calcite, in subordinate quantity – magnetite, potassium feldspar and plagioclase. The two samples are collected from two separate archaeological sites, located in regions with different geological settings. On site No. 8 Dimitriev (sample No. 62), Neogene gravels, sands, and clays outcrop on the earth’s surface

[Boyanov et al., 1991], and on site No. 6 Malko Tranovo (sample No. 83) - Oligocene limestones [Boyanov et al., 1993]. The geological setting explains the presence of calcite in large quantities in sample No. 83 and the lack of it in sample No. 62 which confirms with high probability the local origin of the raw clays used.

Clays in nature are usually bright in colour – white, light beige, light grey [Chamley, 1989; Goffer, 2007]. Both analysed samples have characteristic colouring – an orange-red colour for No. 62 and a bright yellow colour – No. 83 (Figs. 1, 2), which is typical for a clay that has undergone thermal treatment. On the other hand, the archaeological observations show that there are no traces of burning at the sites, which indicates an intentional implementation of a thermal process.

The rich orange-red colour of No.62 is related to the proven hematite in the sample. Despite the fact that the hematite is in low quantity, under 5% is enough for it to give such a colour to the ceramic – even 1 – 1.5% of hematite colours the ceramic intensely [Palanivel et al., 2009]. Sample No. 83 is coloured in bright yellow. No hematite was found in this sample but there is a very large amount of calcite – 20.8%. A ceramic made from calcareous clay is usually in such colours, regardless of the thermal treatment's temperature [Kornilov, 2005].

Ceramic's thermal treatment temperature can be determined by judging its phase composition and by the conducted thermal studies. Feldspars were established in the samples, which are resistant up to around 1200°C [Papadoloulu et al., 2006]. Quartz transitions into tridymite at ~840°C but it can be registered in the samples through PXRD until about 1100°C [Bitay et al., 2020]. Calcite decarbonizes between 750 and 820°C [Böke et al., 2006]. The minerals illite and muscovite undergo a few thermal transformations during heating: dehydration, dehydroxylation, structure destruction, with the last one being an irreversible reaction [Muller et al., 2000; Kotryová et al., 2016]. Through thermal analysis the following is established: decarbonization temperature and destruction temperature of the clay minerals (Table 3) which shows that the samples have not been heated above 808.4°C (No. 83) and above 811.8°C (No. 62). The decomposition temperature of the organic phases cannot be used to determine the heating temperature because the organics may have entered the samples at a much later stage than their production. A magnetite-hematite transition was recorded in both samples (Fig 7,8), which suggests that the thermal treatment temperature of these samples has not reached such high values. FTIR bands at ~1035 cm⁻¹ and ~520 cm⁻¹ of clays - illite and montmorillonite are diagnostic of their heating temperature [Yan et al., 2021]. Bands at 1035 cm⁻¹ and 520 cm⁻¹ are established when heating to 300-400°C. When treating thermally above these temperatures, bands at 1035 cm⁻¹ shift to 1040 cm⁻¹, while band at 520 cm⁻¹ disappears. In sample No. 83 these bands are registered at 1035 cm⁻¹ and 520 cm⁻¹ (Table 2), which suggests a maximum heating of this sample in the specified interval. A band at 526 cm⁻¹ is also found in sample No. 62, but a shift of the band at 1035 cm⁻¹ to 1042 cm⁻¹ is established as well (Table 2). This result indicates with high probability that the heating temperature is also in the range of 300-400°C. On the other hand, goethite is proven in sample No. 62 (Fig. 3), whose structure breakdown temperature (dehydroxylation) is about 300°C [Foldivari, 2010]. In relation to this, it can be assumed that 300°C is also the maximum heating temperature of sample No. 62.

Conclusion

By characterizing the studied Roman wall plasters, the clay types and their treatment method for obtaining the final building ceramic material were determined. Two different types of raw clay were used: non-calcareous clay for sample No. 62 and calcareous clay for sample No.

83, where the clay type determines the final color of the plasters. A low-temperature heat treatment was applied to the raw clays, up to 300°C for No. 62, and between 300 - 400°C for No. 83.

The two types of clay used correspond with the rocks that outcrop on the earth's surface at both archaeological sites, which proves with high probability the use of local raw materials. The thermal treatment with approximately the same temperature is an indication for the use of the same approach when preparing the samples. This approach provided increased strength, which in turn increased the plaster's resistance in time.

The obtained results are of fundamental value, showing a good knowledge of the environment during the Roman Age and an ability to use different natural resources. The application of the same methods was a strong prerequisite for achieving sustainable results. The characterization of ancient plasters also has practical value – the results can be used for the creation of modern building materials, as well as for restoration and conservation of archaeological sites.

Funding

This work was funded by the Bulgarian Science Research Fund - grant number KP-06-N39/9.

Acknowledgments

The authors gratefully acknowledge the Bulgarian Science Research Fund for funding this work (V.I., B.K. – members of the project's team, K. M. – student at the Department of Natural Sciences with a thesis on the subject of the project), as well as New Bulgarian University, the Department of Natural Sciences and the Geology laboratory – BF.

Author contributions: All authors contributed to the study conception and design. Sample collection were performed by B. K. Material preparation were performed by V. I. Thermal analysis data collection were performed by B. K. XRF, PXRD and FTIR analysis were processed and interpreted by B. K. Thermal analysis process and interpretation – by K. M. and V. I. The first draft of the manuscript was written by K. M. and B. K. and all authors commented on previous versions of the manuscript. All authors read and approved the final manuscript.

Conflict of interest: The authors declared no conflict of interest.

REFERENCES

- Aras, A., S. Kiliç, 2017. The mineralogy and firing behaviour of pottery clays of the Lake Van region, eastern Turkey. *Clay Minerals*, 52 (4), 453-468. <https://doi.org/10.1180/claymin.2017.052.4.04>
- Badica, P., A. Alexandru- Dinu, M. A. Grigoroscuta, M. Burdusel, G. V.Aldica, V. Sandu, C. Bartha, S. Polosan, A. Galatanu, V. Kuncser, M. Enculescu, C. Locovei, I. Porosnicu, I.Tiseanu, M. Ferbinteanu, I. Savulescu, M. Negru, N. D. Batalu, 2022. Mud and burnt Roman bricks from Romula. *Scientific Reports*, 12:15864. <https://doi.org/10.1038/s41598-022-19427-7>

- Bayazit, M., I. Işık, A. Issi, E. Genç, 2014. Spectroscopic and thermal techniques for the characterization of the first millennium AD potteries from Kuriki-Turkey. *Ceramics International*, 40 (9-B), 14769-14779. <http://dx.doi.org/10.1016/j.ceramint.2014.06.068>.
- Bitay, E., Kacsó I, Tănăselia C, Toloman D, Borodi G, Pánczél S-P, Kisfaludi-Bak Z, Veress E., 2020. Spectroscopic Characterization of Iron Slags from the Archaeological Sites of Brâncoveneşti, Călugăreni and Vătava Located on the Mureş County (Romania) Sector of the Roman Limes. *Applied Sciences*, 10 (15):5373. <https://doi.org/10.3390/app10155373>
- Boyanov, I., 2014. *Discoduraterae and emporia in Roman Thrace*. Avalon. 232 pp.
- Boyanov, I., A. Goranov, J. Shilyafova, M. Ruseva, 1991. Geolojki karti na Bulgaria, M 1:100000, Karten list Dimitrovgrad. [Geological maps of Bulgaria, M 1:100000, Map sheet Dimitrovgrad].
- Boyanov, I., J. Shilyafova, A. Goranov, M. Ruseva, T. Nenov, 1993. Geolojki karti na Bulgaria, M 1:100000, Karten list Chirpan. [Geological maps of Bulgaria, M 1:100000, Map sheet Chirpan].
- Böke, H., S. Akkurt, B. İpekoğlu, E. Uğurlu, 2006. Characteristics of brick used as aggregate in historic brick-lime mortars and plasters. *Cem Concr Res*, 36 (6), 1115-1122. <https://doi.org/10.1016/j.cemconres.2006.03.011>
- Brown, M. E., P. K. Gallacher (Eds.), 2003. *Handbook of Thermal analysis and Calorimetry. Vol. 2. Applications to inorganic and miscellaneous materials*. Elsevier. 905.
- Chamley, H., 1989. *Clay Sedimentology*. Springer-Verlag Berlin Heidelberg. 623. <https://doi.org/10.1007/978-3-642-85916-8>
- Chukanov, N. V., 2014. *Infrared spectra of mineral species: Extended library*. Springer Geochemistry/Mineralogy, Springer Dordrecht Heidelberg New York London, ISBN: 978-94-007-7127-7, 978-94-007-7128-4.
- Chukanov, N. V., A. D. Chervonnyi, 2016. *Infrared Spectroscopy of Minerals and Related Compounds*. Springer New York Dordrecht London. <https://doi.org/10.1007/978-3-319-25349-7>
- Dumanov, B., 2005. Spasitelni arheologicheski prouchvaniya na obekt № 13a (kusnoantichno selishte) pri s. Malko Tranovo, obshtina Chirpan, po traseto na AM “Trakiya” – LOT 1. [Archaeological rescue research of site № 13a (late antique settlement) near the village Malko Tranovo, Chirpan municipality, along the route of “Trakiya” highway – LOT 1] *Arheologicheski razkopki prez 2004*. [Archaeological excavations in 2004], 243-244.
- El Ouahabi, M., L. Daoudi, F. Hatert, N. Fagel, 2015. Modified Mineral Phases During Clay Ceramic Firing. *Clays Clay Miner.*, 63, 404-413. <https://doi.org/10.1346/CCMN.2015.0630506>
- Emami, M., Y. Sakali, Ch. Pritzel, R. Trettin, 2016. Deep inside the ceramic texture: A microscopic–chemical approach to the phase transition via partial-sintering processes in ancient ceramic matrices. *Journal of Microscopy and Ultrastructure*, 4, 11-19. <http://dx.doi.org/10.1016/j.jmau.2015.08.003>..
- Földvári, M., 2011. *Handbook of the thermogravimetric system of minerals and its use in geological practice*. Occasional Papers of the Geological Institute of Hungary. Budapest. <https://doi.org/10.1556/ceugeol.56.2013.4.6>
- Emiroğlu, M., A. Yalama, Y. Erdoğan, 2015. Performance of ready-mixed clay plasters produced with different clay/sand ratios. *Journal of Applied Clay Science*, 115, 221-229. <https://doi.org/10.1016/j.clay.2015.08.005>

- Goffer, Z., 2007. *Archaeological chemistry*. John Wiley & Sons, Inc., Hoboken, New Jersey. 623.
- Grim, R. E., W. F. Bradley, 1940. Investigation of the effect of heat on the clay minerals illite and montmorillonite. *Journal of the American Ceramic Society*, 23 (8), 242-248. <https://doi.org/10.1111/j.1151-2916.1940.tb14263.x>
- Hatakeyama, T., Zk. Liu, 1998. *Handbook of thermal analysis*. Sussex, England, John Wiley & Sons Ltd. Pp 452.
- Imman, S., P. Khongchamnan, W. Wanmolee, N. Laosiripojana, T. Kreetachat, Ch. Akulthaew, Ch. Chokeyaroenrat, N. Suriyachai, 2021. Fractionation and characterization of lignin from sugarcane bagasse using a sulfuric acid catalyzed solvothermal process. *RSC Advances*, 43 (11). <https://doi.org/10.1039/D1RA03237B>
- Jozanikohan, G., M. Abarghoeei, 2022. The Fourier transform infrared spectroscopy (FTIR) analysis for the clay mineralogy studies in a clastic reservoir. *Journal of Petroleum Exploration and Production Technology*. <https://doi.org/10.1007/s13202-021-01449-y>
- Kotryová, B., J. Ondruška, I. Štubňa, P. Bačík, 2016. Thermoanalytical investigation of ancient pottery. *AIP Conference Proceedings*, 1752, 040016. <https://doi.org/10.1063/1.4955247>
- Kornilov, A. V., 2005. Reasons for the different effects of calcareous clays on strength properties of ceramics. *Glass Ceram*, 62, 391–393. <https://doi.org/10.1007/s10717-006-0017-9>.
- La Noce, M., A. Lo Faro, G. Sciuto, 2021. Clay-Based Products Sustainable Development: Some Applications. *Sustainability*, 13, 1364. <https://doi.org/10.3390/su13031364>
- Laufek, F., I. Hanusová, J. Svoboda, R. Vašíček, J. Najser, M. Koubová, M. Čurda, F. Ptíčen, L. Vaculíková, H. Sun, D. Mašín, 2021. Mineralogical, Geochemical and Geotechnical Study of BCV 2017 Bentonite -The Initial State and the State following Thermal Treatment at 200°C. *Minerals*, 11(8), 871. <https://doi.org/10.3390/min11080871>
- Lee, W.E., G. P. Souza, C. J. McConville, T. Tarvornpanich, Y. Iqbal, 2008. Mullite formation in clays and clay-derived vitreous ceramics. *Journal of the European Ceramic Society*, 28, 465–471. <https://doi.org/10.1016/j.jeurceramsoc.2007.03.009>.
- Lišková, B., P. Jelínek, M. Ostrý, 2016. Impact of hydrophobic additives on properties of clay plaster. *Applied Mechanics and Materials*, 824, 92-99. <https://doi.org/10.4028/www.scientific.net/amm.824.92>
- Ma, X., G. Wei, C. Grifa, Y. Kang, H. Khanjian, I. Kakoulli, 2018. Multi-analytical Studies of Archaeological Chinese Earthen Plasters: The Inner Wall of the Longhu Hall (Yuzhen Palace, Ancient Building Complex, Wudang Mountains, China). *Archaeometry*, 60 (1), 1-18. <https://doi.org/10.1111/arcm.12318>
- Marsh, A., A. Heath, P. Patureau, M. Evernden, P. Walker, 2018. Alkali activation behavior of un-calcined montmorillonite and illite clay minerals. *Applied Clay Science*, 166, 250-261, <https://doi.org/10.1016/j.clay.2018.09.011>
- Melià, P., G. Ruggieri, S. Sabbadini, G. Dotelli, 2014. Environmental impacts of natural and conventional building materials: a case study on earth plasters. *Journal of Cleaner Production*, 80, 179-186, <https://doi.org/10.1016/j.jclepro.2014.05.073>.
- Meyers, K. S., R. F. Speyer, 2003. *Thermal analysis of clays*. In: Brown ME, Gallacher PK, editors. *Handbook of Thermal analysis and Calorimetry*. 2. Applications to inorganic and miscellaneous materials. Amsterdam: Elsevier, pp 268-289.
- Moropoulou, A., A. Bakolas, K. Bisbikou, 1995. Characterization of ancient, byzantine and later historic mortars by thermal and X-ray diffraction techniques. *Thermochimica Acta*, 2570, 743-753. [https://doi.org/10.1016/0040-6031\(95\)02571-5](https://doi.org/10.1016/0040-6031(95)02571-5)

- Muller, F., V. Drits, A. Plançon, J-L. Robert, 2000. Structural Transformation of 2:1 Dioctahedral Layer Silicates during Dehydroxylation-Rehydroxylation Reactions. *Clays Clay Miner*, 48, 572–585. <https://doi.org/10.1346/CCMN.2000.0480510>
- Palanivel, R., U. Rajesh Kumar, 2011. Thermal and spectroscopic analysis of ancient potteries. *Romanian Journal of Physics*, 56 (1-2), 195-208. ISSN 1221-146X.
- PDF (Powder Diffraction File), 2001. ICDD, Newtown Square, PA
- Pei, Z, M. Lin, Y. Liu, S. Lei, 2018. Dissolution Behaviors of Trace Muscovite during Pressure Leaching of Hydrothermal Vein Quartz Using H₂SO₄ and NH₄Cl as Leaching Agents. *Minerals*. <https://doi.org/10.3390/min8020060>
- Ponomar, V. P., 2018. Thermomagnetic properties of the goethite transformation during high-temperature treatment. *Minerals Engineering*, 127, 143-152. <https://doi.org/10.1016/j.mineng.2018.08.016>.
- Rao, H., Y. Yang, X. Hu, J. Yu, H. Jiang, 2017. Identification of an Ancient Birch Bark Quiver from a Tang Dynasty (A.D. 618–907) Tomb in Xinjiang, Northwest China. *Econ Bot*, 71, 32-44. <https://doi.org/10.1007/s12231-017-9369-z>
- Ravisankar, R., S. Kiruba, P. Eswaran, G. Senthilkumar, A. Chandrasekaran, 2010. Mineralogical Characterization Studies of Ancient Potteries of Tamilnadu, India by FT-IR Spectroscopic Technique. *Journal of Chemistry*, 7, 643218, <https://doi.org/10.1155/2010/643218>
- Silva, A., H. R. Wenk, P. J. M. Monteiro, 2005. Comparative investigation of mortars from Roman Colosseum and cistern. *Thermochimica Acta*, 438 (1-2), 35-40. <https://doi.org/10.1016/j.tca.2005.03.003>
- Stanienda, K.J., 2016. Carbonate phases rich in magnesium in the Triassic limestones of the eastern part of the Germanic Basin. *Carbonates Evaporites*, 31, 387-405, <https://doi.org/10.1007/s13146-016-0297-2>
- Singha, M., L. Singh, 2016. Vibrational spectroscopic study of muscovite and biotite layered phyllosilicates. *Indian Journal of Pure & Applied Physics*, 54, 116-122.
- Theophanides, T. (Ed.), 2012. *Infrared Spectroscopy - Materials Science, Engineering and Technology*. London, United Kingdom, IntechOpen. <https://doi.org/10.5772/2055>
- Theodosoglou, E., A. Koroneos, T. Soldatos, T. Zorba, K. M. Paraskevopoulos, 2010. *Bulletin of the Geological Society of Greece, Proceedings of the 12th International Congress Patras, May, 2010. XLIII*, No 5, 2752 – 2761.
- Trindade, M. J., M. I. Dias, J. Coroado, F. Rocha, 2009. Mineralogical transformations of calcareous rich clays with firing: A comparative study between calcite and dolomite rich clays from Algarve, Portugal. *Applied Clay Science*, 42 (3-4), 345-355. <https://doi.org/10.1016/j.clay.2008.02.008>.
- Velosa, A. L., J. Coroado, M. R. Veiga, F. Rocha, 2007. Characterisation of roman mortars from Conímbriga with respect to their repair. *Mater Charact.*, 58 (11-12), 1208-1216. <https://doi.org/10.1016/j.matchar.2007.06.017>
- Yan, B., S. Liu, M. L. Chastain, Sh. Yang, J. Chen, 2021. A new FTIR method for estimating the firing temperature of ceramic bronze-casting moulds from early China. *Sci Rep.*, 11, 3316. <https://doi.org/10.1038/s41598-021-82806-z>